Preprints of the 21st IFAC World Congress (Virtual)
Berlin, Germany, July 12-17, 2020

A Speed Regulator for A Torque–Driven Inertia Wheel Pendulum ⋆

Jesús Sandoval, * **Rafael Kelly** ** **Víctor Santibáñez** *** **Javier Moreno–Valenzuela** ****

* *Tecnológico Nacional de México, Instituto Tecnológico de La Paz, La Paz, B.C.S., 23080 México (e-mail: jesus.sg@lapaz.tecnm.mx).*
** *División de Física Aplicada, CICESE, Ensenada, B.C., 22800 México, (e-mail: rkelly@cicese.edu.mx)*
*** *Tecnológico Nacional de México, Instituto Tecnológico de La Laguna, Torreón, Coahuila, 27001 México, (e-mail: vsantiba@itlalaguna.edu.mx)*
**** *Instituto Politécnico Nacional, CITEDI, Tijuana, B.C., 22435 México, (e-mail: moreno@citedi.mx)*

Abstract: In this paper, we present a speed regulator for a torque–driven inertia wheel pendulum. The proposed controller allows bringing the nonactuated pendulum towards its upright position, while the wheel moves asymptotically at desired constant speed, recovering the popular position regulation control objective for both pendulum and wheel when the desired wheel speed is zero. Also, a complete stability analysis based on the Lyapunov theory and the Barbashin–Krasovskii theorem is presented. Simulation results upon a torque–driven inertia wheel pendulum model illustrate the performance of the proposed controller.

Keywords: Underactuated mechanical systems, coordinates transformation, Barbashin–Krasovskii's theorem, stability.

1. INTRODUCTION

The position regulation (drive all generalized positions to constants values) for a class of underactuated mechanical systems available in many laboratories of automatic control mainly to carry out research –popular simple toy–like mechanisms are those equipped with some non actuated joints– has been solved successfully through several controller design methodologies (e.g., Ortega et al. (2002); Bloch et al. (2000)). The inertia wheel pendulum belong at this class of underactuated mechanical systems and is often used as a benchmark to validate different nonlinear and linear control algorithms (e.g., Ortega et al. (2002); Moreno-Valenzuela & Aguilar-Avelar (2018); Santibáñez et al. (2005)). Furthemore, this underactuated system offers the challenge to control the inverted position of the pendulum by means of a control action driving the unique actuator located in the wheel.

On the other hand, beyond position control schemes for underactuated mechanical systems, there is a few available information dealing with speed regulation of this class of systems. Unlike the fully actuated mechanical systems where speed regulation is related with to aim that all joints of mechanical system track a desired speed, for underactuated mechanical systems we wish that actuated joints follow a desired speed while those underactuated joints go to a proper constant position. At the best knowledge of the authors, at present time a PID controller reported in Romero et al. (2016) is the unique approach solving the speed regulation problem for a class of underactuated mechanical systems, because the work published by Delgado & Kotyczka (2016) deals only with a wheeled inverted pendulum. This PID controller is able to track constant speed trajectories in the actuated joints with constant positions in the underactuated ones. However, the unique example developed lacks of stability analysis. More specifically, in Proposition 4 (Romero et al. (2016), page 3555) the authors claim that the equilibrium point of interest may be almost globally asymptotically stable if a proper output for the closed-loop system is *detectable.* Unfortunately, in the example worked out by the authors the asymptotic stability analysis is ommitted and there is not a guideline or any procedure in order to prove *detectability* from the above output.

The contribution of the present paper is a speed regulator for a torque–driven inertia wheel pendulum. The design approach of the proposed controller is based upon a proper change of coordinates. Moreover, we show a complete stability analysis based on the Lyapunov theory.

Throughout this paper, we use the notation $(\cdot)_{2\times 2}$ to indicate a 2×2 matrix, with $I_{2\times 2}$ as the identity matrix and $0_{2\times 2}$ the matrix of zeros; while $\mathbf{0}_2 \in \mathbb{R}^n$ is the 2×1 vector of zeros, $\nabla_{(\cdot)} = \frac{\partial}{\partial(\cdot)}$, and $\det[A]$ denotes the determinant of the square matrix A.

The remaining of the paper is organized as follows. In Section 2, we present an approach to design a speed regulator of the inertia wheel pendulum, together with the

⋆ This work was partially supported by CONACyT grants 166636, 166654 and 134534, and by TecNM Projects.

stability analysis. Simulation results upon an inertia wheel pendulum are shown in Section 3. Finally, we offer some concluding remarks in Section 4.

2. A TORQUE–DRIVEN INERTIA WHEEL PENDULUM

The torque–driven *inertia wheel pendulum* is an underactuated mechanical system consisting of a physical frictionless pendulum with a symmetric disk (wheel) attached to the tip, which is free to spin about an axis parallel to the axis of rotation of the pendulum (see Figure 1).

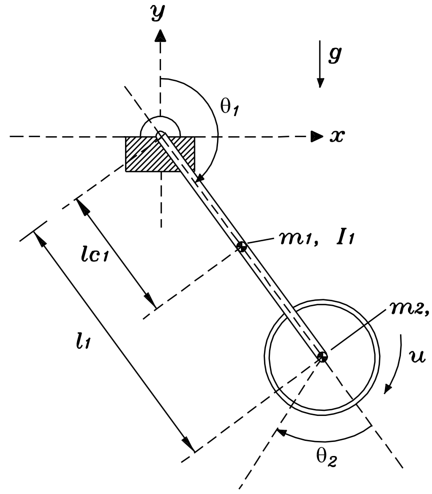

Fig. 1. Sketch of a torque–driven inertia wheel pendulum.

2.1 Control problem formulation

Following the IDA-PBC method introduced by Ortega et al. (2002), the formulation begins with a Hamiltonian–like mathematical description of the torque–driven inertia wheel pendulum, where the energy function (Hamiltonian) is the sum of the kinetic energy plus energy potential of the mechanical system

$$H(\boldsymbol{q},\boldsymbol{p}) = \frac{1}{2}[a_1p_1^2 + 2a_2p_1p_2 + a_3p_2^2] + m_3[\cos(q_1) - 1], \tag{1}$$

where $\boldsymbol{q} = [q_1 \quad q_2]^T$ and $\boldsymbol{p} = [p_1 \quad p_2]^T$ are the vectors of generalized positions and momenta, respectively, the M inertia matrix is given by

$$M = \begin{bmatrix} a_1 & a_2 \\ a_2 & a_3 \end{bmatrix}, \tag{2}$$

and the potential energy function

$$\mathcal{U}(q_1, q_2) = m_3[\cos(q_1) - 1] \tag{3}$$

being $a_1 = I_1 + I_2$, $a_2 = I_2$, $a_3 = I_2$, $m_3 \overset{\triangle}{=} g(m_1l_{c_1} + m_2l)$, and it is defined

$$\begin{bmatrix} q_1 \\ q_2 \end{bmatrix} = \begin{bmatrix} \theta_1 \\ \theta_2 \end{bmatrix} \tag{4}$$

where we have considered $(I_1 + I_2) >> (m_1l_{c_1}^2 + m_2l^2)$ such as the authors did in Ortega et al. (2002) in order to simplify the model. From Figure 1, θ_1 and θ_2 are the joint positions of the pendulum and the wheel, respectively, and u is the control torque input acting between wheel and pendulum. Following the same assumption made in Ortega et al. (2002), it has been assumed both mechanism joints without friction. The meaning of the remaining variables is listed in Table 1.

Table 1. Parameters of the inertia wheel pendulum

Description	Notation	Unit
Length of the pendulum	l_1	m
Distance at the center of mass of the pendulum	l_{c1}	m
Mass of the pendulum	m_1	kg
Mass of the disk	m_2	kg
Moment of inertia of the pendulum	I_1	kg.m^2
Moment of inertia of the disk	I_2	kg.m^2
Gravity acceleration	g	m/s^2

It is important to recall that in Hamiltonian formulation the momentum $\boldsymbol{p}$ is defined as (Nijmeijer & Van der Schaft (1990)):

$$\boldsymbol{p} = M\dot{\boldsymbol{q}} \tag{5}$$

where $\dot{\boldsymbol{q}}$ is the vector of generalized velocities. We assume that the dynamic model of the torque–driven inertia wheel pendulum without viscous friction, can be written as

$$\frac{d}{dt}\begin{bmatrix} \boldsymbol{q} \\ \boldsymbol{p} \end{bmatrix} = \begin{bmatrix} 0_{2\times2} & I_{2\times2} \\ -I_{2\times2} & 0_{2\times2} \end{bmatrix}\begin{bmatrix} \nabla_{\boldsymbol{q}}H(\boldsymbol{q},\boldsymbol{p}) \\ \nabla_{\boldsymbol{p}}H(\boldsymbol{q},\boldsymbol{p}) \end{bmatrix} + \begin{bmatrix} \boldsymbol{0}_2 \\ G \end{bmatrix} u \tag{6}$$

where

$$G = \begin{bmatrix} 0 \\ 1 \end{bmatrix}, \tag{7}$$

and u is the torque control input. Considering (1), (2) and (3) into (6) yields

$$\frac{d}{dt}\begin{bmatrix} q_1 \\ q_2 \\ p_1 \\ p_2 \end{bmatrix} = \begin{bmatrix} \dfrac{[a_3p_1 - a_2p_2]}{\det[M]} \\ \dfrac{[-a_2p_1 + a_1p_2]}{\det[M]} \\ m_3\sin(q_1) \\ u \end{bmatrix} \tag{8}$$

The control problem consists in to find a control law to compute the torque control action u such that substituting into the dynamic model (8) we get the following desired closed-loop system:

$$\frac{d}{dt}\begin{bmatrix} \boldsymbol{q}_a \\ \boldsymbol{p}_a \end{bmatrix} = \begin{bmatrix} 0_{2\times2} & I_{2\times2} \\ -I_{2\times2} & -D_a \end{bmatrix}\begin{bmatrix} \nabla_{\boldsymbol{q}_a}H_a(\boldsymbol{q}_a,\boldsymbol{p}_a) \\ \nabla_{\boldsymbol{p}_a}H_a(\boldsymbol{q}_a,\boldsymbol{p}_a) \end{bmatrix} \tag{9}$$

where we have introduced the coordinates transformation:

$$\boldsymbol{q}_a = K[\boldsymbol{q} - \boldsymbol{q}_d(t)], \tag{10}$$

$$\boldsymbol{p}_a = M_a\dot{\boldsymbol{q}}_a, \tag{11}$$

where K is a 2×2 arbitrary diagonal positive definite constant matrix, $M_a \in \mathbb{R}^{2\times2}$ is an adequate symmetric and positive definite constant matrix, and the "desired" trajectories vector function $\boldsymbol{q}_d(t) \in \mathbb{R}^2$ is a continuous and twice differentiable vector function limited for purposes of constant speed regulation as follows:

$$\boldsymbol{q}_d(t) = [0 \;\; rt]^T \tag{12}$$

where r is the desired wheel speed, and $t \in \mathbb{R}^+$ is the time independent variable, respectively. The position regulation is recovered with $r = 0$, that is, for this case the desired wheel speed is zero. Also, in accordance to (12) it is possible to obtain the desired velocity vector given by

$$\dot{\boldsymbol{q}}_d(t) = [0 \ r]^T, \tag{13}$$

such that,

$$\ddot{\boldsymbol{q}}_d(t) = [0 \ 0]^T. \tag{14}$$

On the other hand, from (10) it follows that

$$\dot{\boldsymbol{q}}_a = K[\dot{\boldsymbol{q}} - \dot{\boldsymbol{q}}_d(t)] \tag{15}$$

and substituting $\dot{\boldsymbol{q}} = M^{-1}\boldsymbol{p}$ and $\dot{\boldsymbol{q}}_a$ from (5) and (15), respectively, into (11), yields

$$\boldsymbol{p}_a = T\boldsymbol{p} - M_a K \dot{\boldsymbol{q}}_d(t) \tag{16}$$

where

$$T = M_a K M^{-1} \tag{17}$$

and rank$(T) = 2$ such that $T^{-1} = MK^{-1}M_a^{-1}$ exists. Continuing with the definitions of the entries in (9), considering (10) and (11), we define the scalar function

$$H_a(\boldsymbol{q}_a, \boldsymbol{p}_a) = \frac{1}{2}\boldsymbol{p}_a^{\mathrm{T}} M_a^{-1} \boldsymbol{p}_a + \mathcal{U}_a(\boldsymbol{q}_a) \tag{18}$$

where $\mathcal{U}_a(\boldsymbol{q}_a)$ is assumed to be a continuously differentiable and locally positive definite function with an isolated minimum point at $\boldsymbol{q}_a = \boldsymbol{0}_2$, which in its turn is a critical point of $\mathcal{U}_a(\boldsymbol{q}_a)$. Finally, we assume that $D_a \in \mathbb{R}^{2\times 2}$ is an arbitrary symmetric positive semi-definite matrix.

For sake of simplicity, from now on, we will denote:
$H = H(\boldsymbol{q}, \boldsymbol{p}), \mathcal{U} = \mathcal{U}(\boldsymbol{q}), H_a = H_a(\boldsymbol{q}_a, \boldsymbol{p}_a), \mathcal{U}_a = \mathcal{U}_a(\boldsymbol{q}_a)$.

2.2 A solution to the control problem

Proposition 1: Consider the dynamic model (6) with (1) and (5). Let M_a, $\mathcal{U}_a$ and $\boldsymbol{q}_d(t)$ solutions of the following equations system

$$G^{\perp}\left[\nabla_{\boldsymbol{q}} H - T^{-1}[\nabla_{\boldsymbol{q}_a} H_a + D_a \nabla_{\boldsymbol{p}_a} H_a]\right] = 0, \tag{19}$$

where $G^{\perp} = [1 \ \ 0^T]$ is a full rank left annhilator of G, that is, $G^{\perp}G = 0$. Then, the desired closed-loop system (9) is achieved via the feedback control law

$$u = [G^T G]^{-1} G^T \left[\nabla_{\boldsymbol{q}} H - T^{-1}[\nabla_{\boldsymbol{q}_a} H_a + D_a \nabla_{\boldsymbol{p}_a} H_a]\right]. \tag{20}$$

$\diamond\diamond\diamond$

Proof: The time derivative $\boldsymbol{p}_a$ from (16) is given by

$$\dot{\boldsymbol{p}}_a = T\dot{\boldsymbol{p}} \tag{21}$$

because M_a and K are constant matrices and $\ddot{\boldsymbol{q}}_d(t) = \boldsymbol{0}_2$ from (14). Substituting $\dot{\boldsymbol{p}}$ from (6) into (21) we obtain

$$\dot{\boldsymbol{p}}_a = T[-\nabla_{\boldsymbol{q}} H + Gu]. \tag{22}$$

Equaling $\dot{\boldsymbol{p}}_a$ from (22) with (9) yields

$$T\left[-\nabla_{\boldsymbol{q}} H + Gu\right] = -\nabla_{\boldsymbol{q}_a} H_a - D_a \nabla_{\boldsymbol{p}_a} H_a \tag{23}$$

which can be written as:

$$-\nabla_{\boldsymbol{q}} H + Gu = T^{-1}[-\nabla_{\boldsymbol{q}_a} H_a - D_a \nabla_{\boldsymbol{p}_a} H_a]. \tag{24}$$

Multiplying both sides of Equation (24) by the invertible matrix $\begin{bmatrix} G^{\perp} \\ G^T \end{bmatrix} = \begin{bmatrix} 1 & 0 \\ 0 & 1 \end{bmatrix}$, results

$$\begin{bmatrix} G^{\perp} \\ G^T \end{bmatrix}\left[-\nabla_{\boldsymbol{q}} H + G\boldsymbol{u}\right] = \begin{bmatrix} G^{\perp} \\ G^T \end{bmatrix} T^{-1}[-\nabla_{\boldsymbol{q}_a} H_a - D_a \nabla_{\boldsymbol{p}_a} H_a] \tag{25}$$

and after some simple calculations allows to obtain the partial differential equation (PDE) defined in (19):

$$G^{\perp}[\nabla_{\boldsymbol{q}} H - T^{-1}[\nabla_{\boldsymbol{q}_a} H_a + D_a \nabla_{\boldsymbol{p}_a} H_a]] = 0, \tag{26}$$

and the control law (20), that is,

$$u = [G^T G]^{-1} G^T [\nabla_{\boldsymbol{q}} H - T^{-1}[\nabla_{\boldsymbol{q}_a} H_a + D_a \nabla_{\boldsymbol{p}_a} H_a]]. \tag{27}$$

Thus, for M_a, $\mathcal{U}_a$ and $\boldsymbol{q}_d(t)$ solutions of (26), the control law (27) substituted into (6) leads to the second row in (9) given by $\dot{\boldsymbol{p}}_a$, that is,

$$\dot{\boldsymbol{p}}_a = -\nabla_{\boldsymbol{q}_a} H_a - D_a \nabla_{\boldsymbol{p}_a} H_a. \tag{28}$$

Next, from (18) we have that

$$\nabla_{\boldsymbol{p}_a} H_a = M_a^{-1} \boldsymbol{p}_a \tag{29}$$

and recalling that (11) is given by $\boldsymbol{p}_a = M_a \dot{\boldsymbol{q}}_a$, substituting into (29), results

$$\nabla_{\boldsymbol{p}_a} H_a = \dot{\boldsymbol{q}}_a. \tag{30}$$

Finally, we conclude that (28) and (30) correspond to (9). This completes the proof.

2.3 Matching equation: potential energy shaping

Since the matrices M and M_a are constant, the expressions $\nabla_{\boldsymbol{q}} H$ and $\nabla_{\boldsymbol{q}_a} H_a$ from (19) may be replaced by $\nabla_{\boldsymbol{q}} \mathcal{U}$ and $\nabla_{\boldsymbol{q}_a} \mathcal{U}_a$, respectively. Moreover, with the end of removing the matrix D_a from (19) in order to facilitate its solution, we choose the T matrix producing a matrix $D_a = D_a^T \geq 0$ defined by:

$$D_a = TGk_v G^T T^T \tag{31}$$

where k_v is an arbitrary strictly positive constant. Then, from (19) the unique PDE set that depends uniquely of $\boldsymbol{q}_a$ and $\boldsymbol{q}_d(t)$ is given by

$$G^{\perp}[\nabla_{\boldsymbol{q}} \mathcal{U} - T^{-1} \nabla_{\boldsymbol{q}_a} \mathcal{U}_a] = 0 \tag{32}$$

being $T^{-1} = MK^{-1}M_a^{-1}$ in accordance with (17). Equation (32) can only be expressed in terms of the $\boldsymbol{q}_a$ variable:

$$G^{\perp} M K^{-1} M_a^{-1} \nabla_{\boldsymbol{q}_a} \mathcal{U}_a = G^{\perp} \nabla_{\boldsymbol{q}} \mathcal{U} \tag{33}$$

once the right-hand side of (33) is first computed and then evaluated for $\boldsymbol{q}_a$ and $\boldsymbol{q}_d(t)$, that is,

$$G^{\perp} \nabla_{\boldsymbol{q}} \mathcal{U}|_{(\boldsymbol{q} = K^{-1}\boldsymbol{q}_a + \boldsymbol{q}_d(t))} \tag{34}$$

where $\boldsymbol{q}$ is written in accordance with (10), and $\boldsymbol{q}_d(t)$ corresponds to (12), such that a solution $\mathcal{U}_a$ may be obtained from (33).

2.4 Control objective: speed regulation

Consider the dynamic model (6) together with the control law (20). We wish that the joint positions $\boldsymbol{q} = [q_1 \quad q_2]^T$ track desired position trajectories $\boldsymbol{q}_d(t) = [0 \quad rt]^T$ asymptotically. Formally, the speed regulation control objective is:

$$\lim_{t\to\infty} [\boldsymbol{q}(t) - \boldsymbol{q}_d(t)] = \mathbf{0}_2. \tag{35}$$

The definition of $\boldsymbol{q}_a$ in (10) allows to rewrite the control objective (35) as follows:

$$\lim_{t\to\infty} \boldsymbol{q}_a(t) = \mathbf{0}_2. \tag{36}$$

We present a solution for the control objective (36) given by the following Proposition.

Proposition 2: Consider the desired closed–loop system (9) and the $\boldsymbol{q}_d(t)$ desired trajectories vector function defined in (12). Consider suitable $M_a = M_a^T > 0$ and proper $\mathcal{U}_a$ is assumed to be a continuously differentiable, and locally positive definite function with an isolated minimum point at $\boldsymbol{q}_a = \mathbf{0}_2$. Let D_a be an arbitrary symmetric positive semi-definite matrix given by (31). Then, the control objective (36) is achieved if the origin $[\boldsymbol{q}_a^T \quad \boldsymbol{p}_a^T]^T = [\mathbf{0}_2^T \quad \mathbf{0}_2^T]^T$ is a locally asymptotically stable equilibrium point.

◇◇◇

Proof: From (9), the origin $[{\boldsymbol{q}_a}^T \quad {\boldsymbol{p}_a}^T]^T = [\mathbf{0}_2^T \quad \mathbf{0}_2^T]^T$ is an isolated equilibrium point. We propose as Lyapunov function the H_a locally positive definite function on a domain $\mathcal{B} \subset \mathbb{R}^4$ defined in (18), whose time derivative along the trajectories of system (9) is given by

$$\dot{H}_a = -\boldsymbol{p}_a^T M_a^{-1} T G k_v G^T T^T M_a^{-1} \boldsymbol{p}_a, \tag{37}$$

which is a negative semidefinite function, because we have selected $D_a = TGK_vG^TT^T \geq 0$, and by design $M_a > 0$ (thus M_a^{-1} is nonsingular). Therefore, this result ensures that the equilibrium point $[{\boldsymbol{q}_a}^T \quad {\boldsymbol{p}_a}^T]^T = [\mathbf{0}_2^T \quad \mathbf{0}_2^T]^T$ is stable. Next, in accordance with the Barbashin–Krasovskii's theorem (Khalil (2002), page 128) we define the S set as:

$$S = \left\{ \boldsymbol{x} \in \mathcal{B} : k_v G^T T^T M_a^{-1} \boldsymbol{p}_a = 0 \right\}, \tag{38}$$

in which we must to prove that no solution can stay identically in S, other than the trivial $[{\boldsymbol{q}_a}^T \quad {\boldsymbol{p}_a}^T]^T = [\mathbf{0}_2^T \quad \mathbf{0}_2^T]^T$ to conclude that the origin is asymptotically stable. This in turn means to demonstrate that the largest invariant set inside S is the origin. Although there is not a general procedure to conclude the above statement, and therefore ensure the control objective (36), inspired in Gandarilla et al. (2019), in this paper we use a strategy for the stability analysis of the torque–driven inertia wheel pendulum, with the end to achieve the control objective (36).

2.5 Control law

The control objective is to drive asymptotically the pendulum to its upright position $q_1 = 0$, and the wheel spinning asymptotically to an arbitrary desired constant speed r. Formally, this goal –which we call position/speed regulation– can be expressed as:

$$\lim_{t\to\infty} \begin{bmatrix} q_1(t) \\ \dot{q}_2(t) \end{bmatrix} = \begin{bmatrix} 0 \\ r \end{bmatrix}, \tag{39}$$

where r is the user free selected desired speed of the wheel (we wish that the wheel tracks the ramp position trajectory $q_2(t) = rt$). The fulfillment of the control objective (36) equals solving the control objective (39) for the inertia wheel pendulum.

In accordance with our approach introduced in Section 2, we propose the coordinates (10)-(11) with K and M_a given by

$$K = \begin{bmatrix} k_1 & 0 \\ 0 & k_2 \end{bmatrix}, \; M_a = \begin{bmatrix} d_1 & d_2 \\ d_2 & d_3 \end{bmatrix}. \tag{40}$$

where we have selected $k_1 = a_1$ and $k_2 = a_2$ to simplify the solution of the PDE in (33), being a_1 and a_2 elements of the M constant matrix from (2). Finally, d_1, d_2 and d_3 are strictly positive constants, where $d_1 > 0$ and $\det[M_a] = d_1 d_3 - d_2^2 > 0$ ensure the possitivity of the M_a matrix.

On the other hand, taking into account that M_a, K and M are matrices with constants elements, the $T = M_a K M^{-1}$ matrix yields

$$T = \frac{1}{\det[M]} \begin{bmatrix} \xi_{11} & \xi_{12} \\ \xi_{21} & \xi_{22} \end{bmatrix} \tag{41}$$

being $\det[M] = a_1 a_3 - a_2^2 > 0$ and the ξ_{ij} constants are:

$$\begin{aligned} \xi_{11} &= d_1 a_1 a_3 - d_2 a_2^2, \; \xi_{12} = -a_1 a_2 [d_1 - d_2], \\ \xi_{21} &= d_2 a_1 a_3 - d_3 a_2^2, \; \xi_{22} = a_1 a_2 [d_3 - d_2]. \end{aligned} \tag{42}$$

Indeed, considering the $G^\perp = [1 \; 0]$ matrix defined in Proposition 1, that is, the PDE in (33) is expressed as:

$$\alpha_1 \frac{\partial \mathcal{U}_a}{\partial q_{a_1}} + \alpha_2 \frac{\partial \mathcal{U}_a}{\partial q_{a_2}} = -m_3 \det[M_a] \sin\left(\frac{q_{a_1}}{a_1} + \bar{q}_{d_1} \right) \tag{43}$$

where $\alpha_1 = [d_3 - d_2]$, $\alpha_2 = [d_1 - d_2]$, and the right-hand side of (43) was computed in accordance with (34), being $q_{d_1}(t) = \bar{q}_{d_1}$ with the constant $\bar{q}_{d_1} \in \{\ldots, -2\pi, 0, 2\pi, \ldots\}$ corresponding to the upright position of the pendulum (see Figure 1). One solution for (43) is given by:

$$\begin{aligned} \mathcal{U}_a = & \frac{a_1 m_3 \det[M_a]}{[d_3 - d_2]} \left[\cos\left(\frac{q_{a_1}}{a_1} + \bar{q}_{d_1} \right) - 1 \right] \\ & + \frac{k_p}{2} [q_{a_2} - \gamma_2 q_{a_1}]^2, \end{aligned} \tag{44}$$

where $\gamma_2 = \frac{(d_1 - d_2)}{(d_3 - d_2)}$, and to guarantee positivity of $\mathcal{U}_a$, the d_i elements are chosen to hold the inequalities:

$$d_1 > d_3, \text{ and } d_2 > d_3, \tag{45}$$

such that $d_1 d_3 - d_2^2 > 0$, and $k_p > 0$. Moreover, $\mathcal{U}_a$ is positive definite with respect to the variables given by $[(q_{a_1} - a_1[\delta\pi - \bar{q}_{d_1}]) \quad (q_{a_2} - \gamma_2 a_1 [\delta\pi - \bar{q}_{d_1}])]^T$ for all δ even, where $\delta \in \mathbb{N}$. Following the notation of Ortega et al. (2002), we write the control law (20) as

$$u = u_{es} + u_{di} \tag{46}$$

where u_{es} is the potential energy shaping term given by

$$\begin{aligned} u_{es} = & [G^T G]^{-1} G^T \left[\nabla_{\boldsymbol{q}} \mathcal{U} - T^{-1} [\nabla_{\boldsymbol{q}_a} \mathcal{U}_a] \right], \\ = & \frac{1}{\det[M_a]} \left[\left[-\frac{a_2}{a_1} d_3 + \frac{a_3}{a_2} d_2 \right] \frac{\partial \mathcal{U}_a}{\partial q_{a_1}} \right. \\ & \left. + \left[\frac{a_2}{a_1} d_2 - \frac{a_3}{a_2} d_1 \right] \frac{\partial \mathcal{U}_a}{\partial q_{a_2}} \right], \end{aligned} \tag{47}$$

with $G^T\nabla_{\boldsymbol{q}}\mathcal{U}=0$ in accordance with (2)-(3), and

$$\frac{\partial\mathcal{U}_a}{\partial q_{a_1}}=-\frac{m_3\det[M_a]}{[d_3-d_2]}\sin\left(\frac{q_{a_1}}{a_1}+\bar{q}_{d_1}\right)-\gamma_2 k_p[q_{a_2}-\gamma_2 q_{a_1}],$$
$$\frac{\partial\mathcal{U}_a}{\partial q_{a_2}}=k_p[q_{a_2}-\gamma_2 q_{a_1}].$$

On the other hand, u_{di} is the damping injection term, simply computed in a such way that

$$\begin{aligned}u_{di}&=-[G^TG]^{-1}G^T[T^{-1}D_a\nabla_{\boldsymbol{p}_a}H_a],\\&=-\frac{k_v a_1 a_2}{\det[M]}[-p_{a_1}+p_{a_2}],\end{aligned}\tag{48}$$

where $D_a=TGK_vG^TT^T$ in accordance with (31) and $T^T=M^{-1}KM_a$.

2.6 Stability analysis

By substituting (46), with (47) plus (48), into (6) and taking into account (10)-(11), the closed-loop system is shown at the top of the next page in Equation (49). It may be verified that the set of equilibria of (49) is

$$\mathcal{E}=\left\{\begin{bmatrix}q_{a_1} & q_{a_2} & p_{a_1} & p_{a_2}\end{bmatrix}^T=\begin{bmatrix}q_{a_1}^* & q_{a_2}^* & 0 & 0\end{bmatrix}^T\in\mathbb{R}^4\right\}$$

where $\boldsymbol{q}_a^*=[q_{a_1}^* \;\; q_{a_2}^*]^T=[a_1[\delta\pi-\bar{q}_{d_1}] \;\; \gamma_2 a_1[\delta\pi-\bar{q}_{d_1}]]^T$ is a minimum of $\mathcal{U}_a(q_{a_1},q_{a_2})$. In acccordance with (39), we consider the origin as the equilibrium of interest, that is, $[q_{a_1}^* \;\; q_{a_2}^*]^T=[0 \;\; 0]^T$ which is achieved with $\bar{q}_{d_1}=\delta\pi$. By simplicity, we have considered $\delta=0$ such that $\bar{q}_{d_1}=0$. Thus, it is convenient to define $\mathcal{B}\subset\mathbb{R}^4$ as

$$\mathcal{B}=\left\{\begin{bmatrix}\boldsymbol{q}_a\\ \boldsymbol{p}_a\end{bmatrix}\in\mathbb{R}^4: q_{a_1}\in\left(-\frac{a_1\pi}{2},\frac{a_1\pi}{2}\right),\; q_{a_2}\in(-\gamma_2 a_1\pi,\gamma_2 a_1\pi)\right\}\tag{50}$$

So, the unique equilibrium in $\mathcal{B}$ is the origin of the state space. Next, we introduce a procedure inspired in the stability analysis developed by Gandarilla et al. (2019) to ensure asymptotic stability of the origin, which is based on the Barbashin–Krasovskii's theorem. Toward this end, we provide the following results. Notice that we can to verify that H_a given by (18) with M_a and $\mathcal{U}_a$ taken from (40) and (44) is a Lyapunov function for (49). It means that H_a is a locally positive definite function and its time derivative along the trajectories of (49) is a negative semi-definite function, given by

$$\dot{H}_a=-k_v\left[\frac{a_1a_2[-p_{a_1}+p_{a_2}]}{\det[M]}\right]^2.$$

Continuing with the steps required by the Barbashin–Krasovskii's theorem, we define the S set as:

$$S=\left\{\begin{bmatrix}\boldsymbol{q}_a\\ \boldsymbol{p}_a\end{bmatrix}\in\mathcal{B}: -p_{a_1}+p_{a_2}=0\right\}.\tag{51}$$

The next step is to prove that no solution can stay identically in S, other than the trivial solution, that is, $[q_{a_1} \;\; q_{a_2} \;\; p_{a_1} \;\; p_{a_2}]^T=[0 \;\; 0 \;\; 0 \;\; 0]^T$. This is equivalent to demonstrate than the largest invariant set into S is this trivial solution. Towards this end, we recall that an invariant set inside of the S set must to accomplish (Haddad & Chellaboina (2008), pp. 147-148):

$$\begin{aligned}\frac{d}{dt}[-p_{a_1}+p_{a_2}]&=0,\\ -\dot{p}_{a_1}+\dot{p}_{a_2}&=0.\end{aligned}\tag{52}$$

Moreover, in accordance with the definiton (11), the equation inside (51) may be rewritten as

$$\dot{q}_{a_2}-\gamma_2\dot{q}_{a_1}=0.$$

Then, by integrating the above equation, it yields

$$\begin{aligned}\int_0^t[\dot{q}_{a_2}(\sigma)-\gamma_2\dot{q}_{a_1}(\sigma)]d\sigma&=0,\\ [q_{a_2}(t)-\gamma_2 q_{a_1}(t)]-\kappa&=0,\\ z(q_{a_1},q_{a_2})-\kappa&=0,\end{aligned}\tag{53}$$

where $z(q_{a_1},q_{a_2})=q_{a_2}(t)-\gamma_2 q_{a_1}(t)$, and the constant κ yields $\kappa=[q_{a_2}(0)-\gamma_2 q_{a_1}(0)]$. Thus, another invariant set belonging at the S set is

$$z(q_{a_1},q_{a_2})=\kappa.\tag{54}$$

In order to simplify our analysis, considering (51) and (54) into (49), we reduce the closed-loop system (49) as follows:

$$\frac{d}{dt}\begin{bmatrix}q_{a_1}\\ q_{a_2}\\ p_{a_1}\\ p_{a_2}\end{bmatrix}=\begin{bmatrix}\dfrac{[d_3-d_2]p_{a_2}}{\det[M_a]}\\ \dfrac{[d_1-d_2]p_{a_2}}{\det[M_a]}\\ \dfrac{m_3\det[M_a]}{[d_3-d_2]}\sin(\dfrac{q_{a_1}}{a_1})-\gamma_2 k_p\kappa\\ -k_p\kappa\end{bmatrix}.\tag{55}$$

From (55), notice that $\dot{p}_{a_2}=-k_p\kappa$, thereby integrating respect to the time is possible to arrive at the next result:

$$p_{a_2}=-k_p\kappa t+C_1,\tag{56}$$

where C_1 is an arbitrary constant. As previously demonstrated the origin is a stable equilibrium point, then the trajectories $[q_{a_1}(t) \;\; q_{a_2}(t) \;\; p_{a_1}(t) \;\; p_{a_2}(t)]^T$ of the closed-loop system (49) starting sufficiently close of the origin, trajectories can be guaranteed to stay within any specified ball centered at the origin, thus inside this region (specified ball centered at the origin) $p_{a_2}(t)$ is bounded (it cannot grow indefinitely with respect to the time), then $\kappa=0$ and this one implies $p_{a_2}=C_1$ and $\dot{p}_{a_2}=0$ from (56) and (55), respectively; from (55) it means that variable p_{a_2} remains constant. Considering the above result into (55) it gets

$$\frac{m_3\det[M_a]}{(d_3-d_2)}\sin\left(\frac{q_{a_1}}{a_1}\right)=0\tag{57}$$

whose unique solution is $q_{a_1}=0$ for $q_{a_1}\in\left(-\frac{a_1\pi}{2},\frac{a_1\pi}{2}\right)$. Replacing $q_{a_1}=0$ and $\kappa=0$ into (54) result $q_{a_2}=0$, which implies $\dot{q}_{a_1}=\dot{q}_{a_2}=0$, and its in turn it gets $p_{a_1}=p_{a_2}=0$. It means that the equilibrium point in the origin $[q_{a_1} \;\; q_{a_2} \;\; p_{a_1} \;\; p_{a_2}]^T=[0 \;\; 0 \;\; 0 \;\; 0]^T$ is the largest invariant set inside the S set. Then, by theorem of Barbashin–Krasovskii we conclude that this equilibrium point is locally asymptotically stable and the control objective (39) is ensured in a local sense.

3. SIMULATION RESULTS

Simulation results upon a torque–driven inertia wheel pendulum model obtained with (2)-(3) by using the parameters given in Ortega et al. (2002) are presented to illustrate the performance of the proposed controller (46), with (47) plus (48). The plant parameters reported in Ortega et al. (2002) are: $I_1=0.1$, $I_2=0.2$ and $m_3=10$. The plant initial configuration considered the

$$\frac{d}{dt}\begin{bmatrix} q_{a_1} \\ q_{a_2} \\ p_{a_1} \\ p_{a_2} \end{bmatrix} = \begin{bmatrix} \frac{1}{\det[M_a]}[d_3 p_{a_1} - d_2 p_{a_2}] \\ \frac{1}{\det[M_a]}[-d_2 p_{a_1} + d_1 p_{a_2}] \\ \frac{m_3 \det[M_a]}{[d_3 - d_2]} \sin\left(\frac{q_{a_1}}{a_1} + \bar{q}_{d_1}\right) + \gamma_2 k_p [q_{a_2} - \gamma_2 q_{a_1}] - \frac{k_v[d_1 - d_2]}{\det[M]}[-p_{a_1} + p_{a_2}] \\ -k_p[q_{a_2} - \gamma_2 q_{a_1}] - \frac{k_v[d_3 - d_2]}{\det[M]}[-p_{a_1} + p_{a_2}] \end{bmatrix} \tag{49}$$

IWP at rest but with a pendulum inclination, that is: $[q_1(0)\ \ q_2(0)\ \ p_1(0)\ \ p_2(0)]^T = [85.9^o\ \ 0\ \ 0\ \ 0]^T$, and a desired constant speed $r = 5$ [rad/s]. The controller gains were set to: $k_p = 0.5$, $k_v = 0.15$, $k_1 = 0.3$, $k_2 = 0.2$, $d_1 = 5$, $d_2 = 2$ and $d_3 = 1$, where the d_i constants fulfill (45). MATLAB software was utilized for numeric simulations with ODE45 solver, which is based on an explicit Runge-Kutta formula, the Dormand-Prince pair, where we have used a relative error tolerance of 1×10^{-3}.

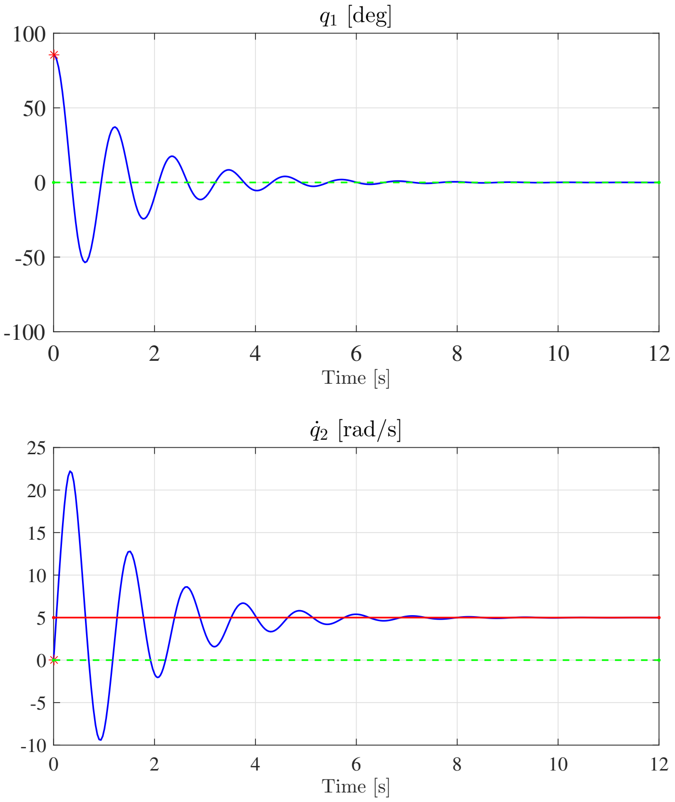

Fig. 2. Time evolution of the joint position of the pendulum q_1 and the wheel speed $\dot{q}_2$.

The plots depicted in Figure 2 show that the joint position q_1 and the wheel speed $\dot{q}_2$ vanish towards the desired values, such that the objective control (39) is achieved.

4. CONCLUSIONS

We have presented a speed regulator for a torque–driven inertia wheel pendulum. A complete analysis in order to prove asymptotic stability of the closed-loop system is developed, such that joint position and constant speed tracking is achieved. Simulations results upon a inertia wheel pendulum model illustrate the performance of the proposed controller.

ACKNOWLEDGEMENTS

The first author thanks Isaac Gandarilla, from Instituto Tecnológico de La Laguna, for his valuable support in the asymptotic stability analysis.

REFERENCES

Acosta, J. A., Ortega, R., Astolfi, A., & Mahindrakar, A. (2005). Interconnection and damping assignment passivity-based control of mechanical systems with underactuation degree one. *IEEE Transactions on Automatic Control*, 50(12), 1936–1955.

Bloch, A. M., Leonard, N. & Marsden, J. (2000). Controlled Lagrangian and the stabilization of mechanical systems. *IEEE Transactions on Automatic Control*, 45(12), 2253–2270.

Delgado, S. & Kotyczka, P. (2016). Energy shaping for position and speed control of a wheeled inverted pendulum in reduced space. *Automatica*, 74, 222–229.

Gandarilla, I., Santibáñez, V. & Sandoval, J. (2019). Control of a self-balancing robot with two degrees of freedom via IDA-PBC. *ISA Transactions*, 88, 102–112.

Haddad, W.,& Chellaboina, V. (2008). *Nonlinear dynamical systems and control.* Princeton, NJ, USA: Princeton University Press.

Khalil, H. K. (2002). *Nonlinear systems* (3rd ed.), Upper Saddle River, NJ, USA: Prentice-Hall.

Moreno-Valenzuela, J. and Aguilar-Avelar, C. (2018). *Motion Control of Underactuated Mechanical Systems* (1st ed.), Springer International Publishing, Cham.

Nijmeijer H. and Van der Schaft A. (1990), *Nonlinear dynamical control systems*, Springer-Verlag New York, USA.

Ortega, R., Spong, M. W., Gómez-Estern, F., & Blankenstein, G. (2002). Stabilization of a class of underactuated mechanical systems via interconnection and damping assignment. *IEEE Transactions on Automatic Control*, 47(8), 1213–1233.

Romero, J., Ortega, R. & Donaire, A. (2016), Energy shaping of mechanical systems via PID control and extension to constant speed tracking, *IEEE Transactions on Automatic Control*, vol. 61, pp. 3551–3556.

Sandoval, J., Kelly, R., & Santibáñez, V. (2011). Interconnection and damping assignment passivity–based control of a class of underactuated mechanical systems with dynamic friction, *International Journal of Robust and Nonlinear Control.* 21(7), 738–751.

Santibáñez, V., Kelly, R. & Sandoval, J. (2005) Control of the inertia wheel pendulum by bounded torques. *In 44th IEEE Conference on Decision and Control and 2005 European Control Conference, CDC-ECC'05* (pp. 8266–8270), Seville, Spain.